This is the Pre-Published Version.

Electronic version of an article published as International Journal of Structural Stability and Dynamics, Vol. 18, No. 08, 1840004 (2018). https://doi.org/10.1142/S0219455418400047. © World Scientific Publishing Company. https://www.worldscientific.com/worldscinet/ijssd.

To: International Journal of Structural Stability and Dynamics

Sensitivity-based finite element model updating using dynamic condensation approach

Tianyi Zhu
Ph.D student,
School of Architecture and Urban Planning,
Huazhong University of Science and Technology
Email: skyspeed@gmail.com

Wei Tian
School of Civil Engineering and Mechanics,
HuazhongUniversity of Science and Technology,
Email: tian_wei@hust.edu.cn

Shun Weng *
School of Civil Engineering and Mechanics,
HuazhongUniversity of Science and Technology,
Wuhan, Hubei, P. R. China
Email: wengshun@mail.hust.edu.cn

Hanbin Ge
Professor
Room 113, Department of Civil Engineering,
Meijo University, Nagoya, Japan
gehanbin@meijo-u.ac.jp

Yong Xia
Professor,
Department of Civil &Environmental Engineering,
The Hong Kong Polytechnic University, Hong Kong
Email: y.xia@polyu.edu.hk

Chao Wang
School of Civil Engineering and Mechanics,
HuazhongUniversity of Science and Technology,
Email:2011210038@qq.com
(* Corresponding author)

Sensitivity-based finite element model updating using dynamic condensation approach

ABSTRACT

An accurate finite element model is frequently used in damage detection, optimization design, reliability analysis, nonlinear analysis and so forth. The finite element model updating of large-scale structures is usually time-consuming or even impossible. This paper proposes a dynamic condensation approach for model updating of large-scale structures. The eigensolutions are calculated from a condensed eigenequation and the eigensensitivities are calculated without selection of additional master DOFs, which is helpful to improve the efficiency of finite element model updating. The proposed model updating method is applied to an eight-storey frame and the JunShanYangtseBridge. By employing the dynamic condensation approach, the number of iterations for the eigensensitivities is gradually increased according to the model updating process, which contributes to accelerate the convergence of model updating.

Keywords: finite element model updating, dynamic condensation approach, eigensolutions, eigensensitivities

1. Introduction

An accurate finite element (FE) model is widely required in the field of damage identification [1, 2], optimization design [3], reliability analysis [4-5], nonlinear analysis [6, 7] and so forth. However, practical applications of FE model often reveal enormous discrepancy between the measured data and the analytical counterpart [8]. An effective model updating method is essential to generate an accurate FE model to estimate the dynamic properties of a practical structure well.

The sensitivity method is probably the most successful one among various FE model updating methods of engineering structures based on the measured dynamic data [9-14]. It adjusts the physical parameters of an analytical FE model iteratively to minimize the discrepancy of dynamic properties between the analytical FE model and the measured counterparts. In the sensitivity method, the eigensolutions are often used to construct the objective function. The eigensensitivities, which are the first order derivatives of the eigensolutions with respect to the designed parameters, indicate a rapid searching direction. As the analytical FE model of a civil structure usually consists of numerous degrees of freedom (DOFs) and uncertain structural parameters, calculations of eigensolutions and associated eigensensitivities based on the large-scale FE model are very time-consuming.

Model condensation selects some DOFs rationally as master DOFs to represent the discarded DOFs (slave DOFs), thus the original model of a large structure is condensed into a much smaller one [15-26]. Since the size of the condensed model is

much smaller than the original full model, calculation of eigensolutions and eigensensitivities based on the condensed model saves plenty of computational resources and time. Since Guyan [15] firstly proposed the static condensation method in 1965, various model condensation methods have been studied, such as the Improved Reduced System (IRS) method [16], the iterated IRS method [17, 18], the Iterative Order Reduction (IOR) method [19, 20] and so on. The model condensation methods have been widely used in extensive applications. He et al. [21] extends the model condensation method to damage detection of continuous bridge combined with Kalman Filtering. Chen et al. [22] proposes a model condensation method to simulate the vertical dynamic behavior of vehicle-track coupled systems efficiently. Weng et al. [23, 24] employs a dynamic condensation approach to calculate the eigensensitivities, structural responses and response sensitivities. Moreover, the efficiency of the model condensation methods can be forwardly improved when combined with the substructuring methods [25-32].

This paper proposes a sensitivity-based FE model updating method using a dynamic condensation approach. The analytical FE model of a structure is condensed into a much smaller one with the dynamic condensation approach. The eigensolutions and eigensensitivities are calculated based on the condensed model to improve their computational efficiency. To improve the computational efficiency of the model updating process, the eigensensitivities are calculated using the proposed dynamic condensation approach without selection of additional master DOFs. Applications of

the proposed method to an eight-storey frame and the JunShanYangtseBridge verify its accuracy and efficiency in dealing with large-scale structures. The number of iterations adopted in the calculation of eigensensitivities is adaptable according to the model updating process, which accelerates the convergence of model updating.

2. Sensitivity-based model updating method

In FE model updating, a residual function is employed to describe the weighted difference between the frequencies and mode shapes gained from the analytical FE model and the corresponding measured data [33, 34]:

$$\begin{aligned} f(\mathbf{r}) &= \left\{ f_\lambda(\mathbf{r}) \quad f_\phi(\mathbf{r}) \right\}^{\mathrm{T}} \\ &= \mathbf{W} \left\{ \lambda_1^A(\mathbf{r}) - \lambda_1^E \quad \cdots \quad \lambda_i^A(\mathbf{r}) - \lambda_i^E \quad \cdots \quad \lambda_n^A(\mathbf{r}) - \lambda_n^E \quad \phi_1^A(\mathbf{r}) - \phi_1^E \quad \cdots \quad \phi_i^A(\mathbf{r}) - \phi_i^E \quad \cdots \quad \phi_n^A(\mathbf{r}) - \phi_n^E \right\}^{\mathrm{T}} \end{aligned} \tag{1}$$

where $\mathbf{r} = \left\{ r_1 \quad \cdots \quad r_{n_r} \right\}^{\mathrm{T}}$ contains the n_r designed physical parameters to be updated. $\lambda_i^A(\mathbf{r})$ and $\phi_i^A(\mathbf{r})$, which are the functions of $\mathbf{r}$ in model updating process, represent the ith (i=1 … n) eigenvalue and eigenvector gained by the analytical FE model, respectively. λ_i^E denotes the ith experimental eigenvalue, which is the square of the circular frequency. ϕ_i^E denotes the ith experimental mode shape. n is the number of modes used for the model updating process. The superscript "T" represents the transpose of a matrix. $\mathbf{W}$ is a diagonal weighting matrixdue to the different measurement accuracy of the eigenvalue and mode shape, which takes the form of

$$\mathbf{W} = \mathrm{Diag}\left[W_{\lambda 1} \quad \cdots \quad W_{\lambda i} \quad \cdots \quad W_{\lambda n} \quad W_{\phi_1} \quad \cdots \quad W_{\phi i} \quad \cdots \quad W_{\phi n} \right] \tag{2}$$

where $W_{\lambda i}$ and $W_{\phi i}$ respectively represent the weighting coefficient of the ith eigenvalue and mode shape.

The FE model updating process is conducted to minimize the square of the norm of $f(\mathbf{r})$ by iteratively adjusting the parameters in $\mathbf{r}$:

$$J(\mathbf{r}) = \min\left(\left\|f(\mathbf{r})\right\|_2^2\right) = \min\left(\left\{f(\mathbf{r})\right\}^{\mathrm{T}}\left\{f(\mathbf{r})\right\}\right) \tag{3}$$

Sensitivity analysis is usually utilized in FE model updating to provide a rapid optimal searching direction [10]. The sensitivity of $f(\mathbf{r})$ with respect to $\mathbf{r}$ is expressed as

$$\mathbf{S}(\mathbf{r}) = \frac{\partial f(\mathbf{r})}{\partial \mathbf{r}} = \mathbf{W}\left[\left\{\frac{\partial f(\mathbf{r})}{\partial r_1}\right\} \quad \cdots \quad \left\{\frac{\partial f(\mathbf{r})}{\partial r_{n_r}}\right\}\right] = \mathbf{W}\begin{bmatrix} \frac{\partial \lambda_1^A(\mathbf{r})}{\partial r_1} & \cdots & \frac{\partial \lambda_1^A(\mathbf{r})}{\partial r_{n_r}} \\ \vdots & & \vdots \\ \frac{\partial \lambda_n^A(\mathbf{r})}{\partial r_1} & \cdots & \frac{\partial \lambda_n^A(\mathbf{r})}{\partial r_{n_r}} \\ \frac{\partial \phi_1^A(\mathbf{r})}{\partial r_1} & \cdots & \frac{\partial \phi_1^A(\mathbf{r})}{\partial r_{n_r}} \\ \vdots & & \vdots \\ \frac{\partial \phi_n^A(\mathbf{r})}{\partial r_1} & \cdots & \frac{\partial \phi_n^A(\mathbf{r})}{\partial r_{n_r}} \end{bmatrix} \tag{4}$$

The eigenvalue and eigenvector derivatives with respect to the designed parameters will be derived with the proposed dynamic condensation approach later.

2.1 Dynamic condensation approach for eigensolutions

The eigenequation of a free undamped structure with N DOFs is expressed as

$$\left(\mathbf{K} - \lambda_i \mathbf{M}\right)\phi_i = \mathbf{0} \tag{5}$$

where $\mathbf{K}$ and $\mathbf{M}$ are respectively the symmetric stiffness and mass matrices of the full model with the size of $N \times N$. λ_i is the ith eigenvalue of the full model, and ϕ_i is the corresponding mode shape. For simplification, λ and ϕ denotes a specific

eigenvalue and mode shape. Hence the subscript "*i*" is deleted hereinafter.

Divide the total DOFs of the structure into n_m master DOFs and n_s slave DOFs, the eigenequation (Eq. (5)) is rewritten as [19, 20]

$$\left(\begin{bmatrix}\mathbf{K}_{mm} & \mathbf{K}_{ms}\\ \mathbf{K}_{ms}^{\mathrm{T}} & \mathbf{K}_{ss}\end{bmatrix}-\lambda\begin{bmatrix}\mathbf{M}_{mm} & \mathbf{M}_{ms}\\ \mathbf{M}_{ms}^{\mathrm{T}} & \mathbf{M}_{ss}\end{bmatrix}\right)\begin{Bmatrix}\phi_m\\ \phi_s\end{Bmatrix}=\begin{Bmatrix}\mathbf{0}\\ \mathbf{0}\end{Bmatrix} \tag{6}$$

where the subscript "*m*" denotes the master DOFs, the subscript "*s*" denotes the slave DOFs, and $N=n_m+n_s$.

According to the second line of Eq. (6), ϕ_s is expressed by ϕ_m as

$$\phi_s=-\left(\mathbf{K}_{ss}-\lambda\mathbf{M}_{ss}\right)^{-1}\left(\mathbf{K}_{ms}^{\mathrm{T}}-\lambda\mathbf{M}_{ms}^{\mathrm{T}}\right)\phi_m \tag{7}$$

A matrix $\mathbf{t}$ is introduced to relate ϕ_s with ϕ_m, which takes the form of

$$\mathbf{t}=-\left(\mathbf{K}_{ss}-\lambda\mathbf{M}_{ss}\right)^{-1}\left(\mathbf{K}_{ms}^{\mathrm{T}}-\lambda\mathbf{M}_{ms}^{\mathrm{T}}\right) \tag{8}$$

As a consequence, the mode shapes of the total DOFs are expressed by those of the master DOFs as

$$\phi=\begin{Bmatrix}\phi_m\\ \phi_s\end{Bmatrix}=\begin{bmatrix}\mathbf{I}_m\\ \mathbf{t}\end{bmatrix}\phi_m=\mathbf{T}\phi_m \tag{9}$$

where $\mathbf{T}$ is the transformation matrix to relate ϕ with ϕ_m, and $\mathbf{I}_m$is a unit matrix with the size of $n_m\times n_m$.

Substituting Eq. (9) into Eq. (5) and premultiplying Eq. (5) with $\mathbf{T}^{\mathrm{T}}$, one can obtain the condensed eigenequation as

$$\left(\mathbf{K}_R - \lambda \mathbf{M}_R\right)\phi_m = \mathbf{0} \tag{10}$$

where $\mathbf{K}_R$ and $\mathbf{M}_R$ are respectively the condensed stiffness and mass matrices, which are expressed as

$$\mathbf{K}_R = \mathbf{T}^{\mathrm{T}}\mathbf{K}\mathbf{T} = \begin{bmatrix}\mathbf{I}_m & \mathbf{t}^{\mathrm{T}}\end{bmatrix}\begin{bmatrix}\mathbf{K}_{mm} & \mathbf{K}_{ms} \\ \mathbf{K}_{ms}^{\mathrm{T}} & \mathbf{K}_{ss}\end{bmatrix}\begin{bmatrix}\mathbf{I}_m \\ \mathbf{t}\end{bmatrix} = \mathbf{K}_{mm} + \mathbf{K}_{ms}\mathbf{t} + \mathbf{t}^{\mathrm{T}}\left(\mathbf{K}_{ms}^{\mathrm{T}} + \mathbf{K}_{ss}\mathbf{t}\right) \tag{10a}$$

$$\mathbf{M}_R = \mathbf{T}^{\mathrm{T}}\mathbf{M}\mathbf{T} = \begin{bmatrix}\mathbf{I}_m & \mathbf{t}^{\mathrm{T}}\end{bmatrix}\begin{bmatrix}\mathbf{M}_{mm} & \mathbf{M}_{ms} \\ \mathbf{M}_{ms}^{\mathrm{T}} & \mathbf{M}_{ss}\end{bmatrix}\begin{bmatrix}\mathbf{I}_m \\ \mathbf{t}\end{bmatrix} = \mathbf{M}_{mm} + \mathbf{M}_{ms}\mathbf{t} + \mathbf{t}^{\mathrm{T}}\left(\mathbf{M}_{ms}^{\mathrm{T}} + \mathbf{M}_{ss}\mathbf{t}\right) \tag{10b}$$

Superior to the original eigenequation (Eq. (5)) with the order of N, the condensed eigenequation (Eq. (10)) has a much smaller order with n_m. The eigensolutions and eigensensitivities calculated from Eq. (10) can improve their computational efficiency greatly. Since $\mathbf{K}_{mm}$, $\mathbf{K}_{ms}$, $\mathbf{K}_{ss}$, $\mathbf{M}_{mm}$, $\mathbf{M}_{ms}$ and $\mathbf{M}_{ss}$ in Eqs. (10a) and (10b) are easily obtained by extracting the associated lines and columns from $\mathbf{K}$ and $\mathbf{M}$ according to the selected master and slave DOFs, only $\mathbf{t}$ is unknown and required to form the condensed eigenequation (Eq. (10)).

Eq. (8) is rewritten by merging the items containing λas

$$\mathbf{t} = -\mathbf{K}_{ss}^{-1}\mathbf{K}_{ms}^{\mathrm{T}} + \lambda\mathbf{K}_{ss}^{-1}\left(\mathbf{M}_{ms}^{\mathrm{T}} + \mathbf{M}_{ss}\mathbf{t}\right) = \mathbf{t}_G + \mathbf{t}_d \tag{11}$$

where

$$\mathbf{t}_G = -\mathbf{K}_{ss}^{-1}\mathbf{K}_{ms}^{\mathrm{T}} \tag{11a}$$

$$\mathbf{t}_d = \lambda\mathbf{K}_{ss}^{-1}\left(\mathbf{M}_{ms}^{\mathrm{T}} + \mathbf{M}_{ss}\mathbf{t}\right) \tag{11b}$$

The subscript "G" represents the variables associated with the Guyan static condensation, which is a constant item gained directly without iteration [15]. The subscript "d" represents a dynamic item in $\mathbf{t}$, which is relevant to λ and achieved by

an iterative process.

Substituting Eqs. (11a), (11b) into Eqs. (10a) and (11b), one can obtain

$$\begin{aligned}\mathbf{K}_R-\lambda\mathbf{M}_R=&\left[\mathbf{K}_{mm}+\mathbf{K}_{ms}\left(\mathbf{t}_G+\mathbf{t}_d\right)\right]+\left(\mathbf{t}_G+\mathbf{t}_d\right)^{\mathrm{T}}\left[\mathbf{K}_{ms}^{\mathrm{T}}+\mathbf{K}_{ss}\left(\mathbf{t}_G+\mathbf{t}_d\right)\right]\\&-\lambda\left\{\mathbf{M}_{mm}+\mathbf{M}_{ms}\left(\mathbf{t}_G+\mathbf{t}_d\right)+\left(\mathbf{t}_G+\mathbf{t}_d\right)^{\mathrm{T}}\left[\mathbf{M}_{ms}^{\mathrm{T}}+\mathbf{M}_{ss}\left(\mathbf{t}_G+\mathbf{t}_d\right)\right]\right\}\\&=\mathbf{K}_G-\lambda\mathbf{M}_d\end{aligned} \tag{12}$$

where

$$\mathbf{K}_G=\mathbf{K}_{mm}+\mathbf{K}_{ms}\mathbf{t}_G \tag{12a}$$

$$\mathbf{M}_d=\mathbf{M}_{mm}+\mathbf{M}_{ms}\mathbf{t}+\mathbf{t}_G^{\mathrm{T}}\left(\mathbf{M}_{ms}^{\mathrm{T}}+\mathbf{M}_{ss}\mathbf{t}\right) \tag{12b}$$

In consequence, Eq. (10) is written as

$$\left(\mathbf{K}_G-\lambda\mathbf{M}_d\right)\phi_m=\mathbf{0} \tag{13}$$

Considering Eq. (13), Eq. (11) can also be rewritten as

$$\mathbf{t}=-\mathbf{K}_{ss}^{-1}\mathbf{K}_{ms}^{\mathrm{T}}+\lambda\mathbf{K}_{ss}^{-1}\left(\mathbf{M}_{ms}^{\mathrm{T}}+\mathbf{M}_{ss}\mathbf{t}\right)=\mathbf{t}_G+\mathbf{K}_{ss}^{-1}\left(\mathbf{M}_{ms}^{\mathrm{T}}+\mathbf{M}_{ss}\mathbf{t}\right)\mathbf{M}_d^{-1}\mathbf{K}_G \tag{14}$$

Afterwards, $\mathbf{t}$ is calculated iteratively based on Eqs. (12b) and (14). Once $\mathbf{t}$ is available, the eigensolutions of the condensed model (λ, ϕ_m) is calculated from Eq. (13) with eigensolver. And the mode shapes of the total DOFs are recovered according to Eq. (9).

2.2. Dynamic condensation approach for eigensensitivities

In this subsection, the dynamic condensation approach is employed to calculate the

first order eigensensitivity with respect to the designed physical parameters **r**. For convenience, a specific parameter *r* from **r** is taken as an illustration.

Differentiating Eq. (10) with respect to *r* gives

$$\left(\mathbf{K}_R - \lambda \mathbf{M}_R\right)\frac{\partial \phi_m}{\partial r} + \left(\frac{\partial \mathbf{K}_R}{\partial r} - \frac{\partial \lambda}{\partial r}\mathbf{M}_R - \lambda \frac{\partial \mathbf{M}_R}{\partial r}\right)\phi_m = \mathbf{0} \tag{15}$$

Pre-multiplying Eq. (15) with ϕ_m^{T} and considering the condensed eigenequation $\left(\mathbf{K}_R - \lambda \mathbf{M}_R\right)\phi_m = \mathbf{0}$ (Eq. (10)) and its orthogonal condition $\phi_m^{\mathrm{T}}\mathbf{M}_R\phi_m = 1$, the eigenvalue derivative is calculated by

$$\frac{\partial \lambda}{\partial r} = \phi_m^{\mathrm{T}}\left(\frac{\partial \mathbf{K}_R}{\partial r} - \lambda \frac{\partial \mathbf{M}_R}{\partial r}\right)\phi_m \tag{16}$$

The eigensolutions of the condensed system (λ, ϕ_m) are calculated in the previous subsection. Therefore, the primary task to obtain the eigenvalue derivatives is to calculate the derivatives of the condensed stiffness and mass matrices ($\frac{\partial \mathbf{K}_R}{\partial r}$ and $\frac{\partial \mathbf{M}_R}{\partial r}$).

Eqs. (10a) and (10b) are differentiated with respect to the elemental parameter *r*

$$\frac{\partial \mathbf{K}_R}{\partial r} = \frac{\partial \mathbf{K}_{mm}}{\partial r} + \frac{\partial \mathbf{K}_{ms}}{\partial r}\mathbf{t} + \mathbf{K}_{ms}\frac{\partial \mathbf{t}}{\partial r} + \frac{\partial \mathbf{t}^{\mathrm{T}}}{\partial r}\left(\mathbf{K}_{ms}^{\mathrm{T}} + \mathbf{K}_{ss}\mathbf{t}\right) + \mathbf{t}^{\mathrm{T}}\left(\frac{\partial \mathbf{K}_{ms}^{\mathrm{T}}}{\partial r} + \frac{\partial \mathbf{K}_{ss}}{\partial r}\mathbf{t} + \mathbf{K}_{ss}\frac{\partial \mathbf{t}}{\partial r}\right) \tag{17}$$

$$\frac{\partial \mathbf{M}_R}{\partial r} = \frac{\partial \mathbf{M}_{mm}}{\partial r} + \frac{\partial \mathbf{M}_{ms}}{\partial r}\mathbf{t} + \mathbf{M}_{ms}\frac{\partial \mathbf{t}}{\partial r} + \frac{\partial \mathbf{t}^{\mathrm{T}}}{\partial r}\left(\mathbf{M}_{ms}^{\mathrm{T}} + \mathbf{M}_{ss}\mathbf{t}\right) + \mathbf{t}^{\mathrm{T}}\left(\frac{\partial \mathbf{M}_{ms}^{\mathrm{T}}}{\partial r} + \frac{\partial \mathbf{M}_{ss}}{\partial r}\mathbf{t} + \mathbf{M}_{ss}\frac{\partial \mathbf{t}}{\partial r}\right) \tag{18}$$

In our previous work in Ref. [23], all DOFs associated with the elemental parameter *r* are selected as the additional master DOFs to localize the effect due to the change of the specific elemental parameter. Consequently, $\frac{\partial \mathbf{K}_{ms}}{\partial r} = \mathbf{0}$, $\frac{\partial \mathbf{K}_{ss}}{\partial r} = \mathbf{0}$, $\frac{\partial \mathbf{M}_{ms}}{\partial r} = \mathbf{0}$

and $\frac{\partial \mathbf{M}_{ss}}{\partial r}=\mathbf{0}$, which is proved to be very efficient in the calculation of eigensensitivities.

However, this simplified method is not efficient to be applied to the FE model updating. In each iteration of the optimal algorithm in FE model updating, the eigensolutions and the eigensensitivities with respect to numerous designed parameters are calculated. Since the additional master DOFs are associated with the designed parameter, the master DOFs of a structure vary in the calculation of eigensensitivities with respect to different designed parameters. In consequence, many intermediate variables generated in the calculation of eigensolutions need to be recalculated for the eigensensitivities. Since most computational resources in the model updating process are consumed on the eigensensitivities [13], the previous method is inefficient to be applied to FE model updating. In addition, the master DOFs are usually rationally selected to calculate the eigensolutions. The additional master DOFs, gathered in the designed element, contaminate the original rational selection of master DOFs. Since improper selection of master DOFs leads to poor eigensolutions and eigensensitivities in dynamic condensation approach, the accuracy and efficiency of the FE model updating is affected greatly [35-37]. Therefore, the additional master DOFs are avoided hereinafter.

In this paper, the master DOFs for eigensensitivity are the same with those for the eigensolution, without all DOFs associated with the elemental parameter *r* included

as additional master DOFs. It is noted from Eqs. (17) and (18) that $\frac{\partial \mathbf{K}_R}{\partial r}$ and $\frac{\partial \mathbf{M}_R}{\partial r}$ are relevant to matrices $\mathbf{K}_{ms}$, $\mathbf{K}_{ss}$, $\mathbf{M}_{ms}$, $\mathbf{M}_{ss}$, $\mathbf{t}$, $\frac{\partial \mathbf{K}_{mm}}{\partial r}$, $\frac{\partial \mathbf{K}_{ms}}{\partial r}$, $\frac{\partial \mathbf{K}_{ss}}{\partial r}$, $\frac{\partial \mathbf{M}_{mm}}{\partial r}$, $\frac{\partial \mathbf{M}_{ms}}{\partial r}$, $\frac{\partial \mathbf{M}_{ss}}{\partial r}$ and $\frac{\partial \mathbf{t}}{\partial r}$. Since matrices $\mathbf{K}_{ms}$, $\mathbf{K}_{ss}$, $\mathbf{M}_{ms}$, $\mathbf{M}_{ss}$ and $\mathbf{t}$ have been calculated for eigensolutions, they are reused here directly. And the derivatives of the stiffness and mass matrices ($\frac{\partial \mathbf{K}_{mm}}{\partial r}$, $\frac{\partial \mathbf{K}_{ms}}{\partial r}$, $\frac{\partial \mathbf{K}_{ss}}{\partial r}$, $\frac{\partial \mathbf{M}_{mm}}{\partial r}$, $\frac{\partial \mathbf{M}_{ms}}{\partial r}$ and $\frac{\partial \mathbf{M}_{ss}}{\partial r}$) are available by extracting the corresponding lines and columns from the specific elemental matrices associated with the selected master and slave DOFs. So the crucial task to calculate the eigensensitivity is to compute $\frac{\partial \mathbf{t}}{\partial r}$.

As $\mathbf{t}$ is estimated iteratively based on Eqs. (12b) and (14), its derivative matrix ($\frac{\partial \mathbf{t}}{\partial r}$) can be achieved iteratively based on the derivatives of Eqs. (12b) and (14) as

$$\frac{\partial \mathbf{M}_d}{\partial r}=\frac{\partial \mathbf{M}_{mm}}{\partial r}+\frac{\partial \mathbf{M}_{ms}}{\partial r}\mathbf{t}+\mathbf{M}_{ms}\frac{\partial \mathbf{t}}{\partial r}+\frac{\partial \mathbf{t}_G^{\mathrm{T}}}{\partial r}\left(\mathbf{M}_{ms}^{\mathrm{T}}+\mathbf{M}_{ss}\mathbf{t}\right)+\mathbf{t}_G^{\mathrm{T}}\left(\frac{\partial \mathbf{M}_{ms}^{\mathrm{T}}}{\partial r}+\frac{\partial \mathbf{M}_{ss}}{\partial r}\mathbf{t}+\mathbf{M}_{ss}\frac{\partial \mathbf{t}}{\partial r}\right) \quad (19)$$

$$\frac{\partial \mathbf{t}}{\partial r}=\frac{\partial \mathbf{t}_G}{\partial r}-\mathbf{K}_{ss}^{-1}\frac{\partial \mathbf{K}_{ss}}{\partial r}\mathbf{K}_{ss}^{-1}\left(\mathbf{M}_{ms}^{\mathrm{T}}+\mathbf{M}_{ss}\mathbf{t}\right)\mathbf{M}_d^{-1}\mathbf{K}_G+\mathbf{K}_{ss}^{-1}\left(\frac{\partial \mathbf{M}_{ms}^{\mathrm{T}}}{\partial r}+\frac{\partial \mathbf{M}_{ss}}{\partial r}\mathbf{t}+\mathbf{M}_{ss}\frac{\partial \mathbf{t}}{\partial r}\right)\mathbf{M}_d^{-1}\mathbf{K}_G$$

$$+\mathbf{K}_{ss}^{-1}\left(\mathbf{M}_{ms}^{\mathrm{T}}+\mathbf{M}_{ss}\mathbf{t}\right)\mathbf{M}_d^{-1}\left(\frac{\partial \mathbf{K}_G}{\partial r}-\frac{\partial \mathbf{M}_d}{\partial r}\mathbf{M}_d^{-1}\mathbf{K}_G\right) \quad (20)$$

Substitute Eq. (14) into Eq. (20), Eq. (20) can be simplified as

$$\frac{\partial \mathbf{t}}{\partial r}=\frac{\partial \mathbf{t}_G}{\partial r}-\mathbf{K}_{ss}^{-1}\frac{\partial \mathbf{K}_{ss}}{\partial r}\left(\mathbf{t}-\mathbf{t}_G\right)+\mathbf{K}_{ss}^{-1}\left(\frac{\partial \mathbf{M}_{ms}^{\mathrm{T}}}{\partial r}+\frac{\partial \mathbf{M}_{ss}}{\partial r}\mathbf{t}+\mathbf{M}_{ss}\frac{\partial \mathbf{t}}{\partial r}\right)\mathbf{M}_d^{-1}\mathbf{K}_G$$

$$+\left(\mathbf{t}-\mathbf{t}_G\right)\mathbf{K}_G^{-1}\left(\frac{\partial \mathbf{K}_G}{\partial r}-\frac{\partial \mathbf{M}_d}{\partial r}\mathbf{M}_d^{-1}\mathbf{K}_G\right) \quad (21)$$

Afterwards, $\frac{\partial \mathbf{t}}{\partial r}$ is achieved iteratively according to Eqs. (19) and (21). Once $\frac{\partial \mathbf{t}}{\partial r}$ is calculated, the eigenvalue derivatives can be achieved based on Eqs. (16)-(18).

The eigenvector derivative with respect to r will be derived based on the condensed eigenequation directly. The eigenvector derivative of the master DOFs is written as the superposition of a particular item and a homogenous item

$$\frac{\partial \phi_m}{\partial r} = \{v\} + c\phi_m \tag{22}$$

where c is a participation factor and $\{v\}$ is a particular item.

Substituting Eq. (22) into Eq. (15) gives

$$\left(\mathbf{K}_R - \lambda \mathbf{M}_R\right)\left(\{v\} + c\phi_m\right) = \left(\frac{\partial \lambda}{\partial r}\mathbf{M}_R + \lambda \frac{\partial \mathbf{M}_R}{\partial r} - \frac{\partial \mathbf{K}_R}{\partial r}\right)\phi_m \tag{23}$$

Since $(\mathbf{K}_R\text{-}\lambda\mathbf{M}_R)\phi_m = \mathbf{0}$ (Eq. (10)), Eq. (23) can be rewritten as

$$\left(\mathbf{K}_R - \lambda \mathbf{M}_R\right)\{v\} = \left(\frac{\partial \lambda}{\partial r}\mathbf{M}_R + \lambda \frac{\partial \mathbf{M}_R}{\partial r} - \frac{\partial \mathbf{K}_R}{\partial r}\right)\phi_m \tag{24}$$

Since $\mathbf{K}_R$, $\mathbf{M}_R$, λ, ϕ_m, $\frac{\partial \mathbf{K}_R}{\partial r}$, $\frac{\partial \mathbf{M}_R}{\partial r}$ and $\frac{\partial \lambda}{\partial r}$ have been computed in the calculation of eigensolutions and eigenvalue derivative, $\{v\}$ can be solved directly from Eq. (24).

The condensed mass matrix $\mathbf{M}_R$ satisfies the orthogonal condition

$$\phi_m^{\mathrm{T}} \mathbf{M}_R \phi_m = 1 \tag{25}$$

Eq. (25) is differentiated with respect to r

$$2\frac{\partial \phi_m^{\mathrm{T}}}{\partial r}\mathbf{M}_R\phi_m + \phi_m^{\mathrm{T}}\frac{\partial \mathbf{M}_R}{\partial r}\phi_m = 0 \tag{26}$$

Substitution of Eq. (22) into Eq. (26) gives

$$2\left(\{v\}^{\mathrm{T}} + c\phi_m^{\mathrm{T}}\right)\mathbf{M}_R\phi_m + \phi_m^{\mathrm{T}}\frac{\partial \mathbf{M}_R}{\partial r}\phi_m = 0 \tag{27}$$

Consequently, the participation factor c is calculated by Eq. (27) as

$$c = -v^{\mathrm{T}}\mathbf{M}_R\phi_m - \frac{1}{2}\phi_m^{\mathrm{T}}\frac{\partial \mathbf{M}_R}{\partial r}\phi_m \tag{28}$$

As $\{v\}$is calculated by Eq. (24) and the participation factor c is calculated by Eq. (28), the eigenvector derivative of the master DOFs ($\frac{\partial \phi_m}{\partial r}$) is available by Eq. (22).

Based on Eqs. (7) and (8), the eigenvector derivative of the slave DOFs ($\frac{\partial \phi_s}{\partial r}$) is calculated by

$$\frac{\partial \phi_s}{\partial r} = \frac{\partial\left(\mathbf{t}\phi_m\right)}{\partial r} = \frac{\partial \mathbf{t}}{\partial r}\phi_m + \mathbf{t}\frac{\partial \phi_m}{\partial r} \tag{29}$$

And the derivative of the eigenvector of the total DOFs is recovered by

$$\frac{\partial \phi}{\partial r} = \begin{Bmatrix} \frac{\partial \phi_m}{\partial r} \\ \frac{\partial \phi_s}{\partial r} \end{Bmatrix} = \begin{bmatrix} \mathbf{0} & \mathbf{I} \\ \frac{\partial \mathbf{t}}{\partial r} & \mathbf{t} \end{bmatrix} \begin{Bmatrix} \phi_m \\ \frac{\partial \phi_m}{\partial r} \end{Bmatrix} \tag{30}$$

3. FE model updating using dynamic condensation approach

Based on the eigensolutions and eigensensitivities calculated by the proposed dynamic condensation approach, the proposed model updating method is performed according to Figure 1.

First, the eigensolutions calculated with the dynamic condensation approach are used to form the objective function. The processes to calculate the eigensolutions are described as follows:

1) **t** is initialized with the Guyan static condensation

$$\mathbf{t}^{[0]} = \mathbf{t}_G = -\mathbf{K}_{ss}^{-1}\mathbf{K}_{ms}^{\mathrm{T}} \tag{31}$$

$$\mathbf{M}_d^{[0]} = \mathbf{M}_G = \mathbf{M}_{mm} + \mathbf{M}_{ms}\mathbf{t}_G + \left(\mathbf{M}_{ms}\mathbf{t}_G\right)^{\mathrm{T}} + \mathbf{t}_G^{\mathrm{T}}\mathbf{M}_{ss}\mathbf{t}_G \tag{32}$$

$$\mathbf{K}_G = \mathbf{K}_{mm} + \mathbf{K}_{ms}\mathbf{t}_G \tag{33}$$

2) **t** is calculated iteratively. In the *k*th (*k*=1, 2, 3 …) iteration,

$$\mathbf{t}^{[k]} = \mathbf{t}_G + \mathbf{K}_{ss}^{-1}\left(\mathbf{M}_{ms}^{T} + \mathbf{M}_{ss}\mathbf{t}^{[k-1]}\right)\left(\mathbf{M}_d^{[k-1]}\right)^{-1}\mathbf{K}_G \tag{34}$$

$$\mathbf{M}_d^{[k]} = \mathbf{M}_{mm} + \mathbf{M}_{ms}\mathbf{t}^{[k]} + \mathbf{t}_G^{\mathrm{T}}\left(\mathbf{M}_{ms}^{\mathrm{T}} + \mathbf{M}_{ss}\mathbf{t}^{[k]}\right) \tag{35}$$

The iteration stops when it reaches the predefined number. And the eigensolutions of the master DOFs are gained by solving the eigenequation

$$\mathbf{K}_G\phi_m = \lambda\mathbf{M}_d\phi_m \tag{36}$$

The mode shapes of the whole DOFs are recovered by those of the master DOFs as

$$\mathbf{T} = \begin{bmatrix} \mathbf{I}_m \\ \mathbf{t} \end{bmatrix} \text{ and } \phi = \mathbf{T}\phi_m \tag{37}$$

3) The weighted differences between the frequencies and mode shapes gained from the measured modal data and the analytical counterpart using the proposed dynamic condensation approach are estimated by the residual function $f(\mathbf{r})$:

$$f(\mathbf{r}) = \mathbf{W}\left\{\lambda_1^A(\mathbf{r}) - \lambda_1^E \quad \cdots \quad \lambda_i^A(\mathbf{r}) - \lambda_i^E \quad \cdots \quad \lambda_n^A(\mathbf{r}) - \lambda_n^E \quad \phi_1^A(\mathbf{r}) - \phi_1^E \quad \cdots \quad \phi_i^A(\mathbf{r}) - \phi_i^E \quad \cdots \quad \phi_n^A(\mathbf{r}) - \phi_n^E\right\}^{\mathrm{T}} \tag{38}$$

The *i*th (*i*=1, 2, 3 … *n*) eigenvalue $\lambda_i^A(\mathbf{r})$ and eigenvectors $\phi_i^A(\mathbf{r})$ of the analytical FE model are calculated using the proposed dynamic condensation approach according to Eq.(36) and Eq.(37).

4) The objective function of the FE model updating is constructed as

$$J(\mathbf{r}) = \min\left(\left\|f(\mathbf{r})\right\|_2^2\right) = \min\left(\left\{f(\mathbf{r})\right\}^T\left\{f(\mathbf{r})\right\}\right) \tag{39}$$

Afterwards, the eigensensitivity calculated by the proposed dynamic condensation approach is used to provide a rapid searching direction for FE model updating.

1) The iteration for eigensensitivity starts with Guyan static condensation

$$\left[\frac{\partial \mathbf{t}}{\partial r}\right]^{[0]}=\frac{\partial \mathbf{t}_G}{\partial r}=\frac{\partial\left(-\mathbf{K}_{ss}^{-1}\mathbf{K}_{ms}^{\mathrm{T}}\right)}{\partial r}=\mathbf{K}_{ss}^{-1}\frac{\partial \mathbf{K}_{ss}}{\partial r}\mathbf{K}_{ss}^{-1}\mathbf{K}_{ms}^{\mathrm{T}}-\mathbf{K}_{ss}^{-1}\frac{\partial \mathbf{K}_{ms}^{\mathrm{T}}}{\partial r}=-\mathbf{K}_{ss}^{-1}\left(\frac{\partial \mathbf{K}_{ss}}{\partial r}\mathbf{t}_G+\frac{\partial \mathbf{K}_{ms}^{\mathrm{T}}}{\partial r}\right) \quad (40)$$

$$\left[\frac{\partial \mathbf{M}_d}{\partial r}\right]^{[0]}=\frac{\partial \mathbf{M}_{mm}}{\partial r}+\frac{\partial \mathbf{M}_{ms}}{\partial r}\mathbf{t}_G+\mathbf{M}_{ms}\frac{\partial \mathbf{t}_G}{\partial r}+\frac{\partial \mathbf{t}_G^{\mathrm{T}}}{\partial r}\left(\mathbf{M}_{ms}^{\mathrm{T}}+\mathbf{M}_{ss}\mathbf{t}_G\right)+\mathbf{t}_G^{\mathrm{T}}\left(\frac{\partial \mathbf{M}_{ms}^{\mathrm{T}}}{\partial r}+\frac{\partial \mathbf{M}_{ss}}{\partial r}\mathbf{t}_G+\mathbf{M}_{ss}\frac{\partial \mathbf{t}_G}{\partial r}\right) \quad (41)$$

$$\frac{\partial \mathbf{K}_G}{\partial r}=\frac{\partial\left(\mathbf{K}_{mm}+\mathbf{K}_{ms}\mathbf{t}_G\right)}{\partial r}=\frac{\partial \mathbf{K}_{mm}}{\partial r}+\frac{\partial \mathbf{K}_{ms}}{\partial r}\mathbf{t}_G+\mathbf{K}_{ms}\frac{\partial \mathbf{t}_G}{\partial r} \quad (42)$$

2) $\frac{\partial \mathbf{t}}{\partial r}$ is calculated iteratively. In the pth (p=1, 2, 3 …) iteration,

$$\left[\frac{\partial \mathbf{t}}{\partial r}\right]^{[p]}=\frac{\partial \mathbf{t}_G}{\partial r}-\mathbf{K}_{ss}^{-1}\frac{\partial \mathbf{K}_{ss}}{\partial r}\left(\mathbf{t}^{[p]}-\mathbf{t}_G\right)+\mathbf{K}_{ss}^{-1}\left(\frac{\partial \mathbf{M}_{ms}^{\mathrm{T}}}{\partial r}+\frac{\partial \mathbf{M}_{ss}}{\partial r}\mathbf{t}^{[p]}+\mathbf{M}_{ss}\left[\frac{\partial \mathbf{t}}{\partial r}\right]^{[p-1]}\right)\left(\mathbf{M}_d^{[p]}\right)^{-1}\mathbf{K}_G$$

$$+\left(\mathbf{t}^{[p]}-\mathbf{t}_G\right)\mathbf{K}_G^{-1}\left(\frac{\partial \mathbf{K}_G}{\partial r}-\left[\frac{\partial \mathbf{M}_d}{\partial r}\right]^{[p-1]}\left(\mathbf{M}_d^{[p]}\right)^{-1}\mathbf{K}_G\right) \quad (43)$$

$$\left[\frac{\partial \mathbf{M}_d}{\partial r}\right]^{[p]}=\frac{\partial \mathbf{M}_{mm}}{\partial r}+\frac{\partial \mathbf{M}_{ms}}{\partial r}\mathbf{t}^{[p]}+\mathbf{M}_{ms}\left[\frac{\partial \mathbf{t}}{\partial r}\right]^{[p]}+\frac{\partial \mathbf{t}_G^{\mathrm{T}}}{\partial r}\left(\mathbf{M}_{ms}^{\mathrm{T}}+\mathbf{M}_{ss}\mathbf{t}^{[p]}\right)$$

$$+\mathbf{t}_G^{\mathrm{T}}\left(\frac{\partial \mathbf{M}_{ms}^{\mathrm{T}}}{\partial r}+\frac{\partial \mathbf{M}_{ss}}{\partial r}\mathbf{t}^{[p]}+\mathbf{M}_{ss}\left[\frac{\partial \mathbf{t}}{\partial r}\right]^{[p]}\right) \quad (44)$$

The iteration stops when it reaches its required number. And the derivatives of the condensed stiffness and mass matrices ($\frac{\partial \mathbf{K}_R}{\partial r}, \frac{\partial \mathbf{M}_R}{\partial r}$) are calculated by

$$\frac{\partial \mathbf{K}_R}{\partial r}=\frac{\partial \mathbf{K}_{mm}}{\partial r}+\frac{\partial \mathbf{K}_{ms}}{\partial r}\mathbf{t}+\mathbf{K}_{ms}\frac{\partial \mathbf{t}}{\partial r}+\frac{\partial \mathbf{t}^{\mathrm{T}}}{\partial r}\left(\mathbf{K}_{ms}^{\mathrm{T}}+\mathbf{K}_{ss}\mathbf{t}\right)+\mathbf{t}^{\mathrm{T}}\left(\frac{\partial \mathbf{K}_{ms}^{\mathrm{T}}}{\partial r}+\frac{\partial \mathbf{K}_{ss}}{\partial r}\mathbf{t}+\mathbf{K}_{ss}\frac{\partial \mathbf{t}}{\partial r}\right) \quad (45)$$

$$\frac{\partial \mathbf{M}_R}{\partial r}=\frac{\partial \mathbf{M}_{mm}}{\partial r}+\frac{\partial \mathbf{M}_{ms}}{\partial r}\mathbf{t}+\mathbf{M}_{ms}\frac{\partial \mathbf{t}}{\partial r}+\frac{\partial \mathbf{t}^{\mathrm{T}}}{\partial r}\left(\mathbf{M}_{ms}^{\mathrm{T}}+\mathbf{M}_{ss}\mathbf{t}\right)+\mathbf{t}^{\mathrm{T}}\left(\frac{\partial \mathbf{M}_{ms}^{\mathrm{T}}}{\partial r}+\frac{\partial \mathbf{M}_{ss}}{\partial r}\mathbf{t}+\mathbf{M}_{ss}\frac{\partial \mathbf{t}}{\partial r}\right) \quad (46)$$

Consequently, the eigenvalue derivative is calculated by

$$\frac{\partial \lambda}{\partial r}=\boldsymbol{\phi}_m^{\mathrm{T}}\left(\frac{\partial \mathbf{K}_R}{\partial r}-\lambda\frac{\partial \mathbf{M}_R}{\partial r}\right)\boldsymbol{\phi}_m \quad (47)$$

Based on Eq. (45), the eigenvalue derivatives of all eigenmodes can be calculated simultaneously by including them in λ and $\boldsymbol{\phi}_m$. It is noted that in each step of the

model updating process, the eigensolutions are calculated once solely while the eigensensitivities are calculated with respect to numerous designed parameters repeatedly. Since the additional master DOFs are avoided in this paper, calculation of the eigensolutions and eigensensitivities share the same master DOFs. In consequence, many intermediate variables generated in the calculation of eigensolutions, for example, $\mathbf{t}$, $\mathbf{t}_G$, $\mathbf{M}_d$, $\mathbf{K}_G$, λ and ϕ_m, are reused directly to compute the eigensensitivities. This significantly contributes to improve the efficiency of the FE model updating of large-scale structures with numerous updating parameters.

3) The eigenvector derivative are calculated based on the condensed stiffness and mass matrices ($\mathbf{K}_R$ and $\mathbf{M}_R$) using Nelson's method [38]. The eigenvector derivative of the master DOFs is

$$\frac{\partial \phi_m}{\partial r} = \{v\} + c\phi_m \tag{48}$$

The eigenvector derivative of the whole DOFs is recovered by that of the master DOFs as

$$\frac{\partial \phi}{\partial r} = \begin{bmatrix} \mathbf{0} & \mathbf{I} \\ \dfrac{\partial \mathbf{t}}{\partial r} & \mathbf{t} \end{bmatrix} \begin{Bmatrix} \phi_m \\ \dfrac{\partial \phi_m}{\partial r} \end{Bmatrix} \tag{49}$$

Finally, the sensitivity-based FE model updating is conducted by iteratively adjusting the parameters $\mathbf{r}$ through optimization algorithms. The elemental parameters are adjusted according to the eigensensitivity, and the FE model updating process stops when the residual function $f(\mathbf{r})$ reaches the predefined tolerance.

4. Case study 1: an eight-storey frame

An eight-storey frame structure (Figure 2) is first employed to verify the accuracy of the proposed method in the calculation of eigensolutions, eigensensitivities and its application to FE model updating. The frame model consists of 160 2D beam elements, 140 nodes and 408 DOFs in total. 16 nodes denoted with red cross in Figure 2 are selected as the master nodes and there are 48 master DOFs in total. Each element has the material constants of bending rigidity (EI) =170×10^6 Nm^2, axial rigidity (EA) =2500×10^6 N, mass per unit length (ρA) =110 kg/m, and Poisson's ratio υ=0.3.

The accuracy of the proposed dynamic condensation approach in the calculation of the eigensolutions and eigensensitivities is first investigated. The first 10 lowest eigensolutions and eigensensitivities with respect to a randomly selected element (Element 100) are calculated following the procedures described in Section 3. The results of the eigensolutions and eigensensitivities using the proposed dynamic condensation approach are listed in Table 1. Five iterations are used to achieve the eigensolutions and eigensensitivity. For comparison, the eigensolutions and eigensensitivities are also calculated with the traditional model updating method performed on the full model, which are taken as the precise values. In the traditional method, the eigensolutions are calculated using the Lanczos method [39] and the eigensensitivities are calculated using the Nelson's method [38]. In Table 1, "Traditional" and "Dynamic" represent the eigensolutions or eigensensitivities

calculated with the traditional method and the proposed dynamic condensation approach, respectively. The MAC values are used to estimate the similarity of mode shapes or eigenvector derivatives between the two methods.

It is obvious from Table 1 that the relative differences of the frequencies as well as the eigenvalue derivatives are much less than 1×10^{-5} for all modes. In addition, the MAC values of the mode shapes and their derivatives are 1.0000 for all modes. Therefore, the proposed dynamic condensation approach is very precise to estimate the eigensolutions and eigensensitivities of the analytical FE model.

In model updating, the elemental parameters are iteratively adjusted to minimize the discrepancies between the modal data gained by the experimental model and the analytical FE model through optimization algorithms. The commonly used Levenberg–Marquardt Method [40] in MATLAB Optimization Function is employed as an optimization algorithm in FE model updating.

The experimental modal data are generated by intentionally reducing the bending rigidities of some elements (as shown in Table 2 and listed in Figure 2) and the model updating is proceeded to identify the reduction. The first 10 lowest eigenvalues and mode shapes calculated from the analytical FE model after reductions are taken as the experimental modal data. They are both used to form the objective function, and the weighting coefficients of the eigenvalues and mode

shapes are respectively 1 and 10. The bending rigidities of all elements are assumed to be the updating parameters and there 160 updating parameters.

The FE model updating is first performed according to State 1 in Table 2 to investigate the accuracy of the proposed dynamic condensation approach on the FE model updating. In State 1, no reductions are imposed on the bending rigidity of any element. The location and severity of reductions identified with the proposed model updating method are displayed in Figure 3(a). It is clear that no obvious reduction of bending rigidity is identified. Therefore, the slight errors of eigensolutions and eigensensitivites introduced by the proposed dynamic condensation approach have little influence on the FE model updating.

In State 2, the bending rigidity of a randomly selected column element (D1 in Figure 1) are intentionally reduced by 30%, while the other elements remain unchanged. The analytical frequencies and mode shapes before and after updating are listed in Table 3. Before model updating, the relative differences between the experimental frequencies and analytical frequencies are more than 0.003 (some even reach 0.01), and only the MAC value of the first mode reach 1.0000. However, after the model updating is conducted, the relative differences between the experimental frequencies and analytical frequencies are nearly 1×10^{-6} mostly and the MAC values reach 1.0000 for all modes. The analytical modal data closely match the experimental counterpart after the proposed model updating process. The location and severity of

the identified reductions of bending rigidity are listed in Figure 3(b). The bending rigidity of Elements 97 and 98 are identified to be reduced by 30%, while no stiffness reduction appears in other elements, which agrees with the intentional stiffness reduction.

Without losing generality, in State 3 the bending rigidity of Elements 97 and 98 are reduced by 30% and the bending rigidity of Elements 131 and 132 are reduced by 25%. Table 4 shows that the relative differences between the experimental frequencies and the analytical frequencies are much more than 0.005 (some even more than 0.015) and only the MAC value of the first mode reaches 1.0000 before model updating. However, after the proposed model updating method is conducted, the relative differences between the experimental and analytical frequencies drop to 1×10^{-7} or less, while the MAC values of all modes reach 1.0000. The location and severity of the discrepancies of bending rigidity are listed in Figure 3(c). It is obvious that the bending rigidity of Element 97 and 98 are identified to be reduced by 30% and the bending rigidity of Element 132 and 133 are identified to be reduced by 25%, while other elements remain unchanged. The identified location and severity of bending rigidity reduction in elemental parameters is in accordance with the assumed ones well.

The identified results in State 2 and State 3 demonstrate that the proposed model updating method is accurate to identify the location and severity of the intentional

bending rigidity reduction. The slight errors introduced by the proposed dynamic condensation approach have little influence on the model updating results.

5. Case study 2: Jun Shan Yangtse Bridge

A practical cable-stayed bridge, Jun Shan Yangtse Bridge in China, is employed here to investigate the accuracy and computational efficiency of the proposed method to practical large-scale structures. The bridge is 4881.178m in length and 33.5m in width. The cable-stayed bridge is modelled by 611 nodes, 758 elements with 3634 DOFs in Figure 4. Six nodes, denoted with red dots and uniformly distributed in the girder, are selected as the master nodes. There are 36 master DOFs in the bridge structure in total.

Similarly, the bending rigidity of 8 elements (denoted with “D” in Figure 4) in the mid-span of the girder are reduced by 30% to generate the experimental modal data. The proposed model updating method is utilized to identify the reductions of bending rigidity. The bending rigidity of all girder elements are selected as the updating parameters and there are 310 updating parameters in total.

The first 10 lowest experimental eigenvalues and mass normalized mode shapes are utilized in the model updating process to construct the objective function. The weighting coefficients of the eigenvalues and mode shapes are 1 and 10, respectively. The sensitivity matrix of the objective function calculated with the proposed dynamic condensation approach is used to offer a rapid searching direction for the

model updating process. The model updating process stops when the objective function is minimized to 1×10^{-9}.

In the dynamic condensation approach, the number of iterations influences the accuracy of eigensensitivities, and consequently, affects the convergence of the model updating process. In model updating process, more accurate eigensensitivities are required if the results are close to the optimum, when small errors in eigensensitivities may lead to an incorrect searching direction. Since the calculation of eigensensitivities consumes most of the computational resources in the FE model updating, the number of iterations for the calculation of eigensensitivities increases gradually according to the progress of the model updating procedure. In the beginning, the eigensensitivities are calculated without iteration, which is equivalent to Guyan static condensation method. Then, the number of iterations increases gradually to achieve a more accurate eigensensitivities as the convergence slows down. In the last few steps, two iterations are used to improve the accuracy of the eigensensitivities and the objective function reaches the predefined tolerance (1×10^{-9}) with 21.01 minutes.

To investigate the efficiency, the traditional model updating method is performed on the full model with the same modal data, convergence criterion and optimization scheme. It takes 39.12 minutes for the objective function to reach the same tolerance. The computational time cost by the proposed method is about 53.71% of that by the

traditional method. The convergence process of the two methods are listed in Figure 5. It is clear that the proposed dynamic condensation-based model updating method and traditional model updating method can both achieve high accuracy in model updating results, while the proposed method converges much faster than the traditional model updating method.

The frequencies and mode shapes, before and after model updating, are compared in Table 5. It is observed that the proposed method can achieve similar results to the traditional method. Table 5 shows that, before model updating, the relative differences of the frequencies are much more than 1×10^{-3} mostly (some even more than 0.01) and only the MAC values of some specific modes (1^{st}, 2^{nd}, and 7^{th}) reach 1.0000. After the model updating process is conducted, the relative differences of frequencies drop sharply to about 1×10^{-6} and the MAC values of all modes reach 1.0000. The location and severity of identified reductions of bending rigidity on the girders are displayed in Figure 6. It is observed that the bending rigidity of the elements in "D" are reduced by 30%, while no obvious reductions are seen in other elements, which agrees with the intentional reductions on the girders. It again proves that the proposed method achieves the same high precision more efficiently than the traditional model updating method.

6. Conclusions

This paper proposes an improved model updating method based on the dynamic condensation approach. The full FE model of a structure is condensed into a much

smaller one with a dynamic condensation approach. The eigensolutions and eigensensitivities are calculated iteratively based on the condensed model. To make the dynamic condensation efficient in model updating, the eigensensitivity is calculated directly without selecting the DOFs of concerned elements as additional master DOFs. Consequently, many intermediate variables generated in the calculation of eigensolutions can be reused directly to gain the eigensensitivities, which saves plenty of computational resources and time in sensitivity-based FE model updating.

The proposed dynamic condensation approach is applied to the FE model updating of an eight-storey frame structure and the Jun Shan Yangtse Bridge. The results of the frame and bridge reveal that the proposed dynamic condensation approach is very precise in the calculation of eignesolutions and eigensensitivities. The slight errors in eigensolutions and eigensensitivities have little influence on the model updating process. Compared to the traditional model updating method performed on the full model, the proposed model updating method converges faster while still achieve the same high precision. The number of iterations are selected in an adaptive manner in the calculation of eigensensitivities to accelerate the model updating process. Applications of the proposed method to the frame and the bridge reveal its accuracy and efficiency in FE model updating process. It can be more promising to be used in large-scale structures combined with substructuring method, which merits future studies.

Acknowledgement

The author would like to acknowledge the support provided by National Natural Science Foundation of China (NSFC, contract number: 51778258,51629801, 51578260), Basic Research Program of China (2016YFC0802002), Fundamental Research Funds of the Central Universities (HUST: 2016JCTD113, 2014TS130 and 2015MS064), and the Research Funds of Wuhan Urban and Rural Construction Commission (201742, 201511 and 201621).

References

[1] D. S. Wang, W. Xiang, P. Zeng and H. P. Zhu, Damage identification in shear-type structures using a proper orthogonal decomposition approach, *J. Sound Vib*. **355** (2015) 135-149.

[2] H. P. Zhu, L. Mao and S. Weng, A sensitivity-based structural damage identification method with unknown input excitation using transmissibility concept, *J. Sound Vib*. **333**(26) (2014) 7135-7150.

[3] H. F. Yin, H. B. Fang, Q. Wang and G. L. Wen, Design optimization of a MASH TL-3 concrete barrier using RBF-based metamodels and nonlinear finite element simulations, *Eng*. *Struct*. **114** (2016) 122-34.

[4] H. A. Jensen, F. Mayorga and C. Papadimitriou, Reliability sensitivity analysis of stochastic finite element models, *Comput. Method. Appl. M*. **296** (2015) 327-351.

[5] D. Q. Li, T. Xiao, Z. J. Cao, C. B. Zhou and L. M. Zhang, Enhancement of random finite element method in reliability analysis and risk assessment of soil slopes using Subset Simulation, *Landslides*. **13**(2) (2016) 293-303.

[6] L. Li, Y. J. Hu and X. L. Wang, A study on design sensitivity analysis for general nonlinear eigenproblems, *Mech. Syst. Signal Pr*. **34** (2013) 88-105.

[7] M. M. Alamdari, J. C. Li, B. Samali, H. Ahmadian and A. Naghavi, Nonlinear joint model updating in assembled structures, *J.Eng. Mech*. **140**(7) (2014) 1-11.

[8] J. E. Mottershead, M. Link and M. I. Friswell, The sensitivity method in finite element model updating: A tutorial, *Mech*. *Syst*. *Signal Pr*. **25** (2011) 2275-2296.

[9] S. S. Law, J. Li and Y. Ding, Structural response reconstruction with transmissibility concept in frequency domain, *Mech*. *SystemsSignalPr*. **25**(3) (2011) 952-968.

[10] J. E. Mottershead and M. I. Friswell, Model updating in structural dynamics: a survey, *J. Sound Vib*. **167**(2) (1993) 347-375.

[11] N. A. Z. Abdullah, M. S. M. Sani, M. M. Rahman and I. Zaman, A review on model updating in structural dynamics, *3rd Int*. *Conf*. *Mech*. *Eng*. *Res*. 2015, Malaysia.

[12] M. I. Friswell and J. E. Mottershead, Finite element model updating in structural dynamics, *Kluwer Academic Publishers*, 1995.

[13] S. Weng, Y. Xia, Y. L. Xu and H. P. Zhu, Substructure based approach to finite element model updating, *Comput*. *Struct*. **89** (2011) 772-782.

[14] S. Weng, H. P. Zhu, Y. Xia, L. Ye and X. Y Hu, Construction of stiffness and flexibility for substructure-based model updating, *Math*. *Probl*. *Eng*. (2013) 1-14.

[15] R. J. Guyan, Reduction of stiffness and mass matrices, *AIAA J*. **3**(2) (1965) 380.

[16] J. O' Callahan, A procedure for an improved reduced system (IRS) model, *The 7th International Modal Anal*ysis *Conference*. 1989, Orlando, FL, USA.

[17] M. I. Friswell, Model reduction using dynamic and iterated IRS techniques, *J. Sound Vib*. **186**(2) (1995) 311-323.

[18] M. I. Friswell, S. D. Garvey and J. E. T. Penny, The convergence of the iterated IRS method, *J. Sound Vib*. **211**(1) (1998) 123-132.

[19] Y. Xia and R. M. Lin, A new iterative order reduction (IOR) method for eigensolutions of large structures, *Int*. *J*. *Numer*. *Meth*. *Eng*. **59**(1) (2004) 153-172.

[20] Y. Xia and R. M. Lin, Improvement on the iterated IRS method for structural eigensolutions, *J. Sound Vib*. **270** (2004) 713-727.

[21] H. X. He, Y. W. Lv and E. Z. Han, Damage detection for continuous bridge based on static-dynamic condensation and extended Kalman filtering, *Math*. *Probl*. *Eng*. (2014) 1-14.

[22] Y. C. Chen, B. J. Zhang, N. Zhang and M. Y. Zheng, A condensation method for the dynamic analysis of vertical vehicle-track interaction considering vehicle flexibility, *J. Vib*. *Acoust*. **137**(4) (2015) 1-8.

[23] S. Weng, A. Z. Zhu, H. P. Zhu, Y. Xia, L. Mao and P. H. Li, Dynamic condensation approach to the calculation of eigensensitivity, *Comput. Struct*. **132** (2014) 55-64.

[24] S. Weng, W. Tian, H. P. Zhu, Y. Xia, F. Gao, Y. T. Zhang and J. J. Li, Dynamic condensation approach to calculation of structural responses and response

sensitivities, *Mech. Syst. Signal Pr*. **88** (2017) 302-317.

[25] Z. S. Liu and Z. G Wu, Iterative-order-reduction substructuring method for dynamic condensation of finite element models, *AIAA J*. **49**(1) (2011) 87-96.

[26] D. Choi, H. Kim and M. Cho, Iterative method for dynamic condensation combined with substructuring scheme, *J. Sound Vib*. **317** (2008) 199-218.

[27] J. Li and H. Hao, Substructure damage identification based on wavelet domain response reconstruction, *Struct. Health Monit.***13**(2014) 389-405.

[28] S. Weng, H. P. Zhu, Y. Xia and L. Mao, Damage detection using the eigenparameter decomposition of substructural flexibility matrix, *Mech. Syst. Signal Pr*. **34** (2013) 19-38.

[29] S. Weng, H. P. Zhu, Y. Xia, X. Q. Zhou and L. Mao, Substructuring approach to the calculation of higher-order eigensensitivity, *Comput. Struct*. **117** (2013) 23-33.

[30] S. Weng, Y. Xia, X. Q. Zhou, Y. L. Xu and H. P. Zhu, Inverse substructure method for model updating of structures, *J. Sound Vib*. **331** (25) (2012) 5449-5468.

[31] S. Weng, Y. Xia, Y. L. Xu and H. P. Zhu, An iterative substructuring approach to the calculation of eigensolution and eigensensitivity, *J. Sound Vib*. **330**(14) (2011) 3368-3380.

[32] Y. Xia, S. Weng, Y. L. Xu and H. P. Zhu, Calculation of eigenvalue and eigenvector derivatives with the improved Kron's substructuring method, *Struct. Eng. Mech*. **36**(1) (2010) 37-55.

[33] G. Boscato, S. Russo, R. Ceravolo and L. Z. Fragonara, Global sensitivity-based model updating for heritage structures, *Comput.-Aided Civ.Inf.***30**(8) (2015) 620-635.

[34] P. G. Bakir, E. Reynders and G. D. Roeck, Sensitivity-based finite element model updating using constrained optimization with a trust region algorithm, *J. Sound Vib*. **305** (2007) 211-225.

[35] K. O. Kim and Y. J. Choi, Energy method for selection of degrees of freedom in condensation, *AIAA J*. **38**(7) (2000) 1253-1259.

[36] M. Cho and H. Kim, Element-based node selection method for reduction of eigenvalue problems, *AIAA J*. **42**(8) (2004) 1677-1684.

[37] J. Jeong, S. Baek and M. Cho, Dynamic condensation in a damped system through rational selection of primary degrees of freedom, *J. Sound Vib*. **331**(7) (2012) 1655-1668.

[38] R. B. Nelson, Simplified calculation of eigenvector derivatives, *AIAA J*. **14**(9) (1976) 1201-1205.

[39] C. Lanczos, An iteration method for the solution of the eigenvalue problem of linear differential and integral operators, *J*. *Res*. *Natl*. *Inst*. *Stan*. **45**(45) (2008) 255-282.

[40] K. Madson, H. B. Nielsen and O. Tingleff, Methods for non-linear least squares problems, *Inform*. *Math*. *Model*. (2004) 1-30.

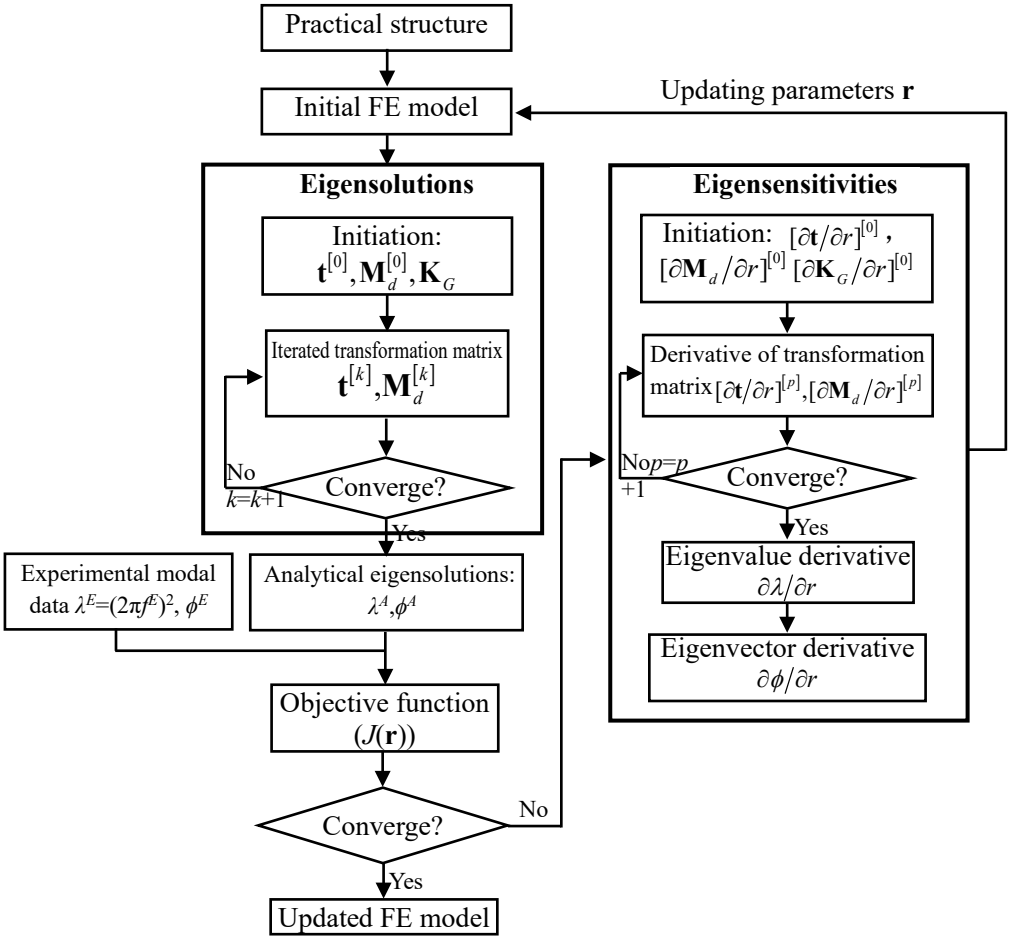

Figure 1. The flowchart of the proposed model updating method.

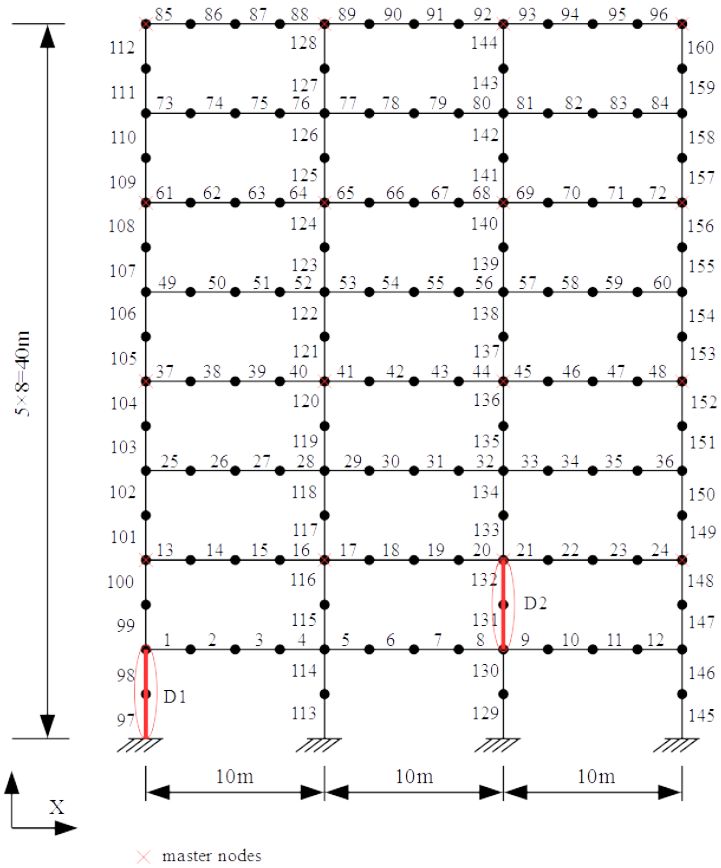

Figure 2. The frame structure.

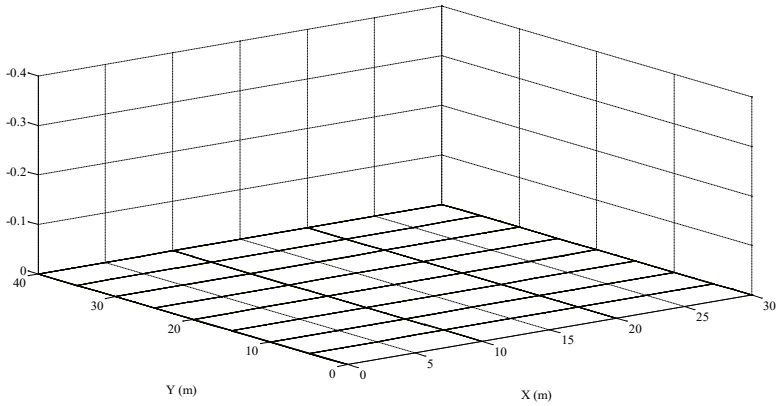

(a) State 1

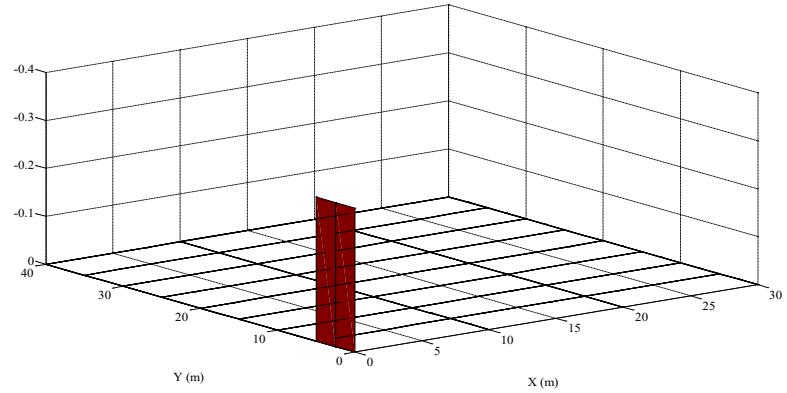

(b) State 2

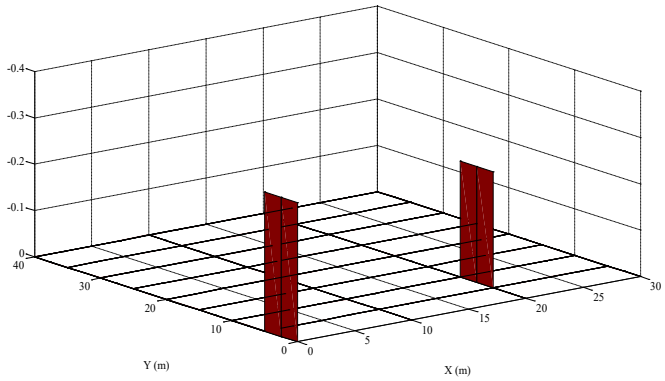

(c) State 3

Figure 3. Location and severity of reductions of bending rigidity identified using the proposed method

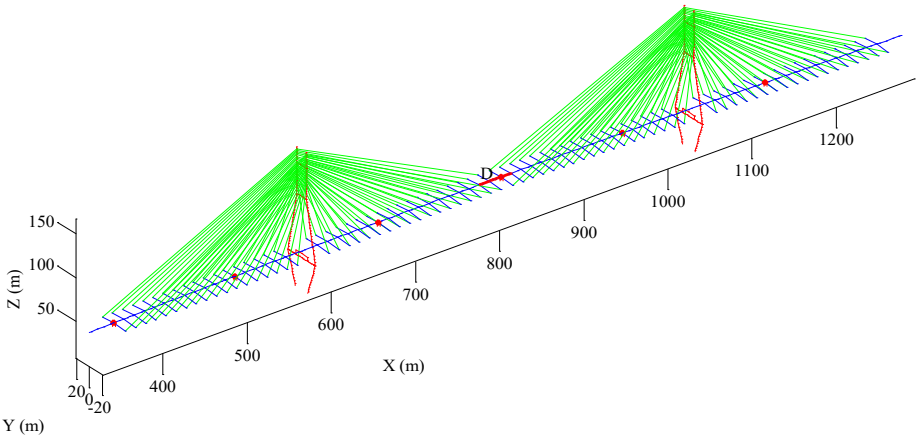

Figure 4. The cable-stayed bridge structure.

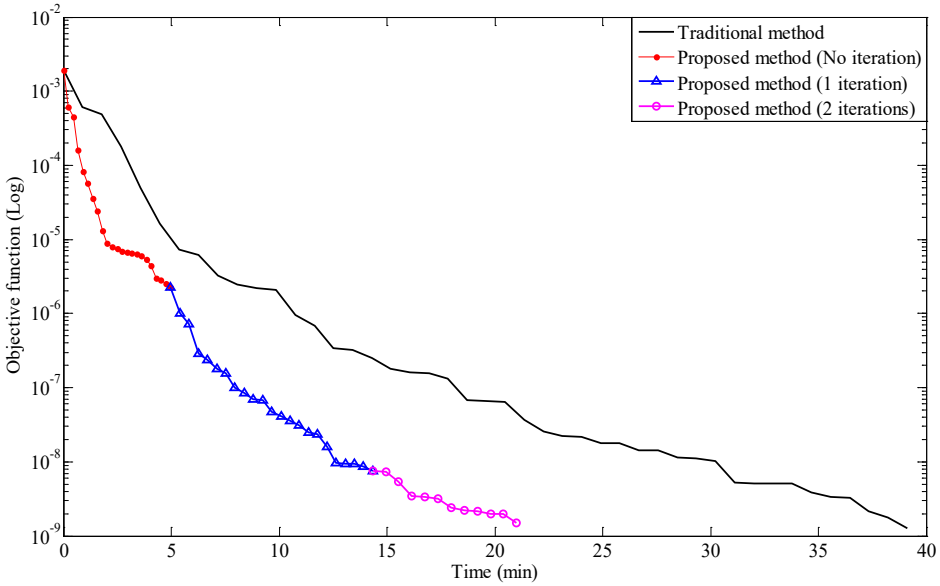

Figure 5. The convergence of model updating with the proposed method and the traditional method

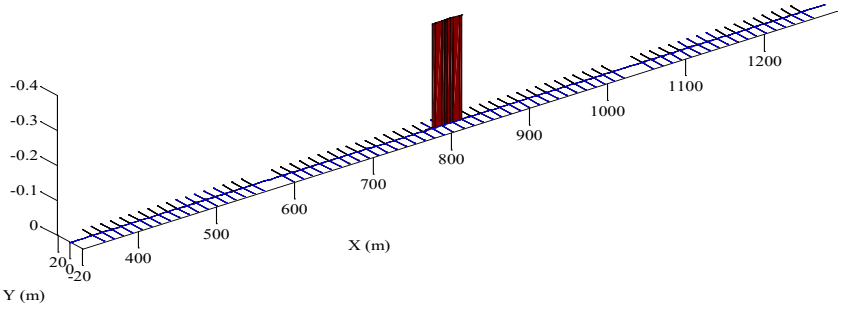

Figure 6. Location and severity of reductions of bending rigidity on the girders identified using the proposed method

Table 1. The eigensolutions and eigensensitivities of the frame using the proposed dynamic condensation approach and the traditional method.

Modes	Eigensolutions				Eigensensitivities			
	Frequencies (Hz)			MAC	Eigenvalue derivatives			MAC
	Traditional	Condensed	Difference		Traditional	Condensed	Difference	
1	1.7844	1.7844	1.199E-11	1.0000	0.6721	0.6721	6.067E-08	1.0000
2	5.5393	5.5393	-7.039E-13	1.0000	7.9383	7.9383	3.207E-09	1.0000
3	9.8308	9.8308	3.872E-11	1.0000	28.5959	28.5959	4.962E-09	1.0000
4	14.7158	14.7158	3.804E-09	1.0000	51.3372	51.3372	9.934E-10	1.0000
5	16.6176	16.6176	1.086E-07	1.0000	72.0617	72.0618	1.088E-07	1.0000
6	18.7967	18.7967	1.790E-07	1.0000	287.1557	287.1556	3.644E-08	1.0000
7	20.2521	20.2521	1.831E-07	1.0000	27.4472	27.4472	1.613E-08	1.0000
8	22.6229	22.6229	8.373E-07	1.0000	717.2171	717.2196	3.503E-06	1.0000
9	25.5300	25.5300	4.485E-07	1.0000	621.0015	621.0017	3.455E-07	1.0000
10	26.2450	26.2451	3.988E-06	1.0000	199.9773	199.9764	4.772E-06	1.0000

Table 2. The intentional reduction of bending rigidity in the elements of the frame.

State	State 1	State 2	State 3
Intentional reduction of bending rigidity	No reduction	Element 97 (-30%) Element 98 (-30%)	Element 97 (-30%) Element 98 (-30%) Element 131 (-25%) Element 132 (-25%)

Table 3. The frequencies and mode shapes of the frame structure before and after model updating (State 2).

Modes	Experimental frequencies (Hz)	Before updating			After updating		
		Analytical frequencies (Hz)	Difference	MAC	Analytical frequencies (Hz)	Difference	MAC
1	1.7760	1.7844	0.004699	1.0000	1.7760	-6.260E-07	1.0000
2	5.5176	5.5393	0.003933	0.9999	5.5176	5.845E-07	1.0000
3	9.7917	9.8308	0.003996	0.9998	9.7917	-3.159E-07	1.0000
4	14.6496	14.7158	0.004517	0.9995	14.6496	5.932E-07	1.0000
5	16.5602	16.6176	0.003467	0.9966	16.5602	-8.967E-07	1.0000
6	18.6054	18.7967	0.01028	0.9912	18.6054	-6.837E-07	1.0000
7	20.1529	20.2521	0.004924	0.9990	20.1529	8.010E-07	1.0000
8	22.2509	22.6229	0.01672	0.9837	22.2509	-7.661E-08	1.0000
9	25.2778	25.5300	0.009976	0.9846	25.2778	-1.024E-06	1.0000
10	26.1035	26.2451	0.005426	0.9961	26.1035	1.603E-06	1.0000

Table 4. The frequencies and mode shapes of the frame structure before and after model updating (State 3).

Modes	Experimental frequencies (Hz)	Before updating			After updating		
		Analytical frequencies (Hz)	Difference	MAC	Analytical frequencies (Hz)	Difference	MAC
1	1.7692	1.7844	0.008584	1.0000	1.7692	-5.627E-08	1.0000
2	5.5019	5.5393	0.006812	0.9999	5.5019	4.847E-08	1.0000
3	9.7783	9.8308	0.005376	0.9997	9.7783	-5.352E-08	1.0000
4	14.6377	14.7158	0.005331	0.9994	14.6377	4.650E-08	1.0000
5	16.3320	16.6176	0.01749	0.9973	16.3320	-1.064E-07	1.0000
6	18.4604	18.7967	0.01822	0.9906	18.4604	-1.108E-07	1.0000
7	20.1075	20.2521	0.007194	0.9980	20.1075	6.364E-08	1.0000
8	22.2349	22.6229	0.01745	0.9847	22.2349	-7.009E-08	1.0000
9	25.1377	25.5300	0.01561	0.9871	25.1376	-1.235E-07	1.0000
10	25.9559	26.2451	0.01114	0.9918	25.9559	1.700E-07	1.0000

Table 5. The frequencies and mode shapes of the cable-stayed bridge before and after model updating.

Modes	Experimental frequencies (Hz)	Before updating			After updating					
					Traditional method			Dynamic condensation method		
		Frequencies (Hz)	Difference	MAC	Frequencies (Hz)	Difference	MAC	Frequencies (Hz)	Difference	MAC
1	0.0095641	0.0095642	1.903E-05	1.0000	0.0095640	-4.045E-06	1.0000	0.0095640	-6.088E-06	1.0000
2	0.018497	0.018744	0.01334	1.0000	0.018497	-8.096E-06	1.0000	0.018497	-7.931E-06	1.0000
3	0.032720	0.032800	0.002446	0.9999	0.032720	-2.116E-06	1.0000	0.032720	-2.639E-06	1.0000
4	0.045195	0.045280	0.001888	1.0000	0.045195	-7.605E-06	1.0000	0.045195	-7.038E-06	1.0000
5	0.055270	0.055333	0.001133	1.0000	0.055270	-6.584E-06	1.0000	0.055270	-8.224E-06	1.0000
6	0.069274	0.069690	0.006010	0.9979	0.069274	-1.371E-07	1.0000	0.069274	2.236E-07	1.0000
7	0.076091	0.076111	0.0002615	1.0000	0.076091	-5.605E-06	1.0000	0.076091	-6.773E-06	1.0000
8	0.082514	0.083299	0.009509	0.9968	0.082515	2.903E-06	1.0000	0.082515	4.341E-06	1.0000
9	0.095127	0.096291	0.01224	0.9985	0.095126	-6.687E-06	1.0000	0.095126	-8.074E-06	1.0000
10	0.099286	0.099494	0.002101	0.9999	0.099285	-6.434E-06	1.0000	0.099285	-4.568E-06	1.0000